



A quantitative model for the geological strength index based on attribute mathematics and its application

Liping Li¹ · Guangyu Yang¹ · Hongliang Liu¹ · Shuguang Song¹ · Hongyun Fan¹

Received: 9 January 2020 / Accepted: 4 July 2021 / Published online: 22 July 2021
© Springer-Verlag GmbH Germany, part of Springer Nature 2021

Abstract

This article introduces a new quantitative model for the geological strength index (GSI) based on attribute mathematics theory. This new attribute evaluation index system of GSI consists of the rock mass block index, the joint spacing, the number of joint sets, the absolute weathering index, the large-scale undulation, and the small-scale undulation. Recently, based on attribute mathematics theory, the attribute mathematics evaluation model of GSI was established for identifying and classifying the geological strength index. Finally, based on the confidence criterion and the method of linear interpolation, a quantitative model for the geological strength index is established. To verify the model, an improved numerical method is introduced. Meanwhile, the equivalent transformation method of the Hoek–Brown strength criterion and Mohr–Coulomb strength criterion is cited. The problems in the determination of the reinforcement time to support surrounding rock are solved by the analysis of the construction process mechanics. A new concept called section displacement deviation is proposed for effective comparison of the monitoring data and the simulation predictions. Project applications prove that this quantitative method has strong pertinence and high accuracy and can organically combine geological surveys, experimental data, statistics, and expert opinions, so this evaluation method can decrease the subjectivity of research decisions. The method of the attribute mathematics evaluation of GSI provides a new approach to quantifying the GSI system.

Keywords GSI · Hoek–Brown · Attribute mathematic · Quantification · Numerical verification

Introduction

A rock mass is a complex geological body composed of structural bodies and structural planes that form in certain geological environments. Due to the existence of discontinuous structures such as joints, cleavages, and faults, the engineering properties of rock masses with discontinuous structures are quite different from those of intact rocks. Limited by the current testing technology, the mechanical parameters of rock masses are difficult to define, so derated mechanical parameters of intact rock are widely used as the basis for estimating rock mass parameters. Hoek et al. proposed the Hoek–Brown strength criterion, which is based on the two major sets of factors of rock mass structural fabric and joint conditions, using the GSI index for the conversion of rock

mechanical parameters to rock mass mechanical parameters (Hoek et al. 1997, 2006).

GSI is a comprehensive reflection of the rock mass structural characteristics and joint conditions. The core of GSI quantification is the construction and quantitative characterization of these two major index factors (Winn et al. 2019), which are the central issues in related research at home and abroad. For example, the GSI parameters of rock mass are quantified (Sonmez and Ulusay 1999, 2002; Sonmez et al. 2004) by introducing the rock mass structure series SR and rock mass surface condition grade, which is based on the joint count of a rock mass volume, and continuously revising and applying the quantified GSI system. Cai et al. (2004, 2006) proposed a quantitative method for determining GSI based on the rock mass volume and the joint condition coefficient, and this method is based on describing geological indexes (such as joint roughness, joint spacing, and filling condition) and field test parameters. Russo (2009) analyzed the relationship between the rock mass block index (RBI) and the rock mass strength parameter formula obtained by the uniaxial compressive strength reduction of intact rock in

✉ Hongliang Liu
sdulihongliang@163.com

¹ Geotechnical and Structural Engineering Research Center, Shandong University, Jinan 250061, China

a GSI system and obtained the relationship between the GSI and the joint condition parameter. Finally, a mixed method for determining the GSI value was proposed with the joint condition parameter as an index. Hoek et al. (2013) proposed quantifying the GSI with the rock quality designation (RQD) and with the joint condition rating of the rock mass rating (RMR) system. Lin et al. (2014) introduced the complete length of the core to quantify the structural information of the rock mass and established a GSI quantification system based on the complete drill core length index and joint conditions by using typical photos of the drill core and joint plane. Schlotfeldt and Carter (2018) introduced the concept of the bias free volumetric fracture count (VFC) parameter in GSI chart quantification, which effectively mitigates the scalability of GSI and the treatment of deviations related to RQD used in the quantification process. A supplementary quantified approach (Feng et al. 2018) for the GSI system was proposed by focusing on the rock mass disturbance factor, which uses the surface condition rating, the structural plane condition factor, the rock mass basic quality index, and the rock mass structure rating. Marinós and Carter (2018) suggested that the ranges in the variability of intact rock parameters σ_{ci} and m_i for common rock masses are presented in the context of a composite new GSI chart, which allows selection of appropriate GSI ranges for any specific rock suite. Although the above quantitative methods can reduce the value error of the GSI system, the GSI values are highly empirical and still need to be further improved.

In this paper, a qualitative–quantitative index system for rock mass structural characteristics and structural plane conditions is established by comprehensively considering the rock mass block index, the joint group number, the joint spacing, the weathering degree of the structural plane, and the roughness degree of the structural plane. The attribute identification model of the GSI system is established to realize attribute interval division of the geological strength index by applying the comprehensive mathematical multi-factor attribute evaluation theory to GSI system evaluation. Then, the concept of confidence ranking is introduced. The minimum confidence ranking and the maximum confidence ranking are taken as endpoint values to realize the on-site quantification of the GSI attribute interval by using linear interpolation. Finally, by further decreasing uncertainty, the attribute quantification model of the geological strength index is constructed to realize the transformation of GSI from attribute interval acquisition to numerical quantification. On the basis of the abovementioned method and referring to the equivalent transformation method of the Hoek–Brown strength criterion and Mohr–Coulomb strength criterion, the effective transformation of rock mechanical parameters to rock mass mechanical parameters in numerical simulation is realized. Compared with the on-site monitoring data, the application effect is discussed. Through this

method, the attribute quantification model of GSI is constructed, and the inconvenience of numerical simulation based on the Hoek–Brown strength criterion is resolved by referring to the equivalent transformation method of the Hoek–Brown strength criterion and Mohr–Coulomb strength criterion. This method can also optimize the values of the numerical simulation calculation parameters, ensure the accuracy of the numerical simulation to a certain extent, and solve the ambiguity of matching monitoring data and numerical simulation predictions with numerical calculation.

Attribute identification model of GSI

Based on the attribute evaluation index system considering the rock mass structure and joint conditions, this article establishes an attribute identification model of GSI. Attribute interval division of the rock mass structure and joint conditions is achieved through three steps: single-index attribute measure analysis, multiple index attribute measure analysis, and attribute identification analysis (Li et al. 2013; Zhou et al. 2013). Finally, the GSI value table proposed by Hoek et al. (2006) is referenced to realize attribute interval discrimination of the GSI.

Referring to the GSI value table (Marinós et al. 2000; Hoek et al. 2013), GSI is mainly affected by the rock mass structure and structural plane surface conditions, as shown in Fig. 1. Let X be the evaluation object and establish the evaluation object space X_i ($i=1,2$) = {rock mass structural characteristics, structural plane surface conditions}. X_1 refers to the arrangement and combination of the rock mass structural planes and structures. At present, there are two main types of descriptions. One is based on rock cores and is usually represented by quantitative indicators such as RQD and RBI. The second is based on the apparent characteristics of the rock mass and is usually expressed by apparent quantitative indicators such as joint group number and spacing. However, it is difficult for any expression form to effectively reflect the three-dimensional structural characteristics of the rock mass.

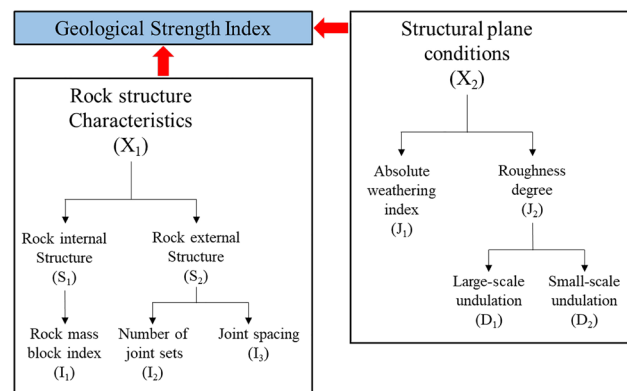


Fig. 1 The GSI attribute identification model

Table 1 Expression of rock-mass structure by RBI (Hu et al. 2002)

| RBI | Qualitative index of rock mass characteristics |
|----------|--|
| A 30~100 | The overall structure, intact or with large blocks, basically has no disturbance, and its integral coefficient is generally greater than 0.75 |
| B 30~10 | The block structure is relatively intact, with no or partial disturbance, and its integral coefficient is generally 0.75–0.55 |
| C 10~3 | The mosaic structure has poor integrity and is generally broken.. However, the rock blocks are stable, and their integral coefficient is generally 0.55~0.35 |
| D 3~1 | Broken structure: the rock mass is broken and fully disturbed, via fractures or thin layers, with well-developed structural planes, and its integrity coefficient is generally 0.35~0.15 |
| E 1~0 | Loose structure: the rock mass is extremely fragmented, disturbed, and loose, and the integrity coefficient is generally less than 0.15 |

Therefore, this article integrates the internal and apparent structural characteristics of a rock mass and constructs an evaluation index system of the rock mass structural characteristics $I_j (j = 1,2,3) = \{\text{rock mass block degree, joint group number, joint spacing}\}$. X_2 refers to the contact state of the structural plane, which directly affects the mechanical properties of the structural plane and is mainly related to the degree of surface weathering, the degree of filling and the surface morphology. This article constructs a surface condition evaluation index system $J_i (i = 1,2) = \{\text{Absolute weathering index, surface roughness degree}\}$. For further description of surface roughness degree, the secondary index is $D_i (i = 1,2) = \{\text{large-scale waveform factor, small-scale waveform factor}\}$. Taking the GSI value table (Hoek et al. 2006), the vertical and horizontal coordinates are divided into five sections. For the measured value t_i of each index, the five-level attribute space $F = \{\text{evaluation grade}\} = C_K (i = 1,2,3,4,5) = \{A, B, C, D, E\}$ is constructed to realize the effective matching between the value section of each index and the coordinate section of the GSI.

Evaluation index system of the rock mass structural attributes

Quantitative index of rock mass internal structure

The RBI is a main indicator of the internal structure of the rock (Hu et al. 2002). It is determined from cores collected perpendicular to the surface of the rock mass. The measured core lengths are taken as weight values according to

the core acquisition rates of the five categories of 3 ~ 10 cm, 10 ~ 30 cm, 30 ~ 50 cm, 50 ~ 100 cm, and more than 100 cm. The cumulative value multiplied by the respective corresponding coefficient is taken as the evaluation index, which is the comprehensive embodiment of the rock mass internal structural characteristics. Referring to Hu et al. (2002), the 5-level attribute space of the RBI index is shown in Table 1.

Quantitative index of rock mass apparent structure

A joint group is the main focus of the rock mass structural surface characteristics and the measurement index of the potential of the rock mass to fragment. It is the comprehensive embodiment of the occurrence and intersection relationship of structural planes. According to previous studies, the more joint groups there are, the more likely the rock mass will be cut into blocks and the higher the degree of rock mass fragmentation. Referring to the research of Bar et al. (2017) and Barton (2002), taking the joint group as the main control factor, the 5-level attribute space of J_n is defined as shown in Table 2.

The joint spacing J_L is the second expression of the rock mass structural surface characteristics. It is the main controlling factor for the integrity of the rock mass and has a certain influence on the volume and quantity of the rock mass. Taking the joint spacing J_L as a parameter, and combining it with the description of the rock mass structural plane number J_n , the comprehensive quantification of the competence and integrity degree can be realized. Based on the research of Bieniawski (1989), the 5-level attribute space of the J_L index is shown in Table 3.

Table 2 Expression of rock mass structure by joint group J_n (Bar et al. 2017; Barton 2002)

| Structure type | J_n | Qualitative index of rock mass characteristics |
|----------------|-----------|---|
| A | 0.5 ~ 1.0 | Massive, no or few joints |
| B | 1.0 ~ 5.0 | One or two sets/one joint set plus random joints |
| C | 5.0 ~ 10 | Three sets/two joint set plus random joints |
| D | 10 ~ 15 | Three joint set plus random joints/four or more joint sets |
| E | 15 ~ 20 | More than four joint sets, random, heavily jointed/ crushed rock, soil-like |

Table 3 Expression of rock mass structure by joint spacing J_L (Bieniawski 1989)

| Structure type | J_L | Rock mass characteristics qualitative indicators |
|----------------|-----------|--|
| A | > 200 cm | Intact or massive, complete rock mass or large-scale distribution with few large-spacing structural planes, generally larger than 200 cm |
| B | 60~200 cm | Blocky, inlaid undisturbed rock mass, and joint spacing is generally greater than 60 cm, less than 200 cm |
| C | 20~60 cm | Very blocky, partial disturbance, and joint spacing is generally not more than 60 cm |
| D | 6~20 cm | Blocky/disturbed/seamy, rock mass is broken and fully disturbed, bedding plane or schistosity plane is developed, and the joint spacing is generally not more than 20 cm |
| E | < 6 cm | Disintegrated, rock mass is extremely broken and mixed, consisting of angular and round rock blocks |

Attribute evaluation index system of structural surface conditions

Quantitative index of weathering filling conditions

The joint condition is a qualitative description of the mechanical properties of the structural plane. The weathering of structural planes will lead to changes in the surface morphology, filling characteristics, contact relationship, and rock mass properties, which will lead to unknown changes in the mechanical properties of the rock mass structural planes. Referring to the research results of Su et al. (2009) and considering the filling state of structural planes, the *AWI* is defined as the weathering and filling degree of the rock mass. The 5-level attribute space of the *AWI* index is shown in Table 4.

Quantitative index of surface roughness

The degree of joint roughness is an important influence parameter in the analysis of the mechanical properties of a structural plane. It directly affects the cohesion and internal friction angle of structural planes and thus influences the shear resistance of the structural planes. According to the research sampling range and referring to the large-scale fluctuation coefficient and small-scale fluctuation coefficient, the roughness of joints is quantified at two scales.

The large-scale wave coefficient J_b is defined as the rate of undulation of the rock mass surface within the range of 1~10 m. According to the fluctuation rate, the 5-level attribute space of the large-scale wave coefficient J_b is shown in Table 5 (Cai et al. 2004). The small-scale wave coefficient J_s is defined as the degree of the rock mass surface smoothness within the range of 1~20 cm. According to the volatility, the 5-level attribute space of the small-scale wave coefficient J_s is shown in Table 6 (Cai et al. 2004).

Analysis of single-index attribute measurement

Based on the above analysis, the rock mass quality evaluation and classification standards are shown in Table 7. There are six evaluation indexes in Table 7 that satisfy the attribute spaces $F = \{\text{structural characteristics of rock mass}\} = \{I_1, I_2, I_3\} = \{\text{RBI}, J_L, J_n\}$, $D = \{\text{roughness of structural surface}\} = \{D_1, D_2\} = \{J_b, J_s\}$, and $S = \{\text{joint condition}\} = \{J, D\} = \{AWI, D\}$. This data satisfy the data format requirements of mathematical attribute calculations. Therefore, attribute operations can be performed on attribute sets, corresponding attribute measures can be given for different attribute sets, and additivity rules can be satisfied. The single-index attribute measure μ_{ijk} expresses the measured value t_j of the J th evaluation index of the I th object in the evaluation object space with the size of the attribute C_k . The size of the I th object with level C_k is expressed by the comprehensive attribute measure

Table 4 Expression of rock mass weathering by *AWI* (Su et al. 2009)

| Structure type | <i>AWI</i> | Rock mass characteristic qualitative indicators |
|----------------|------------|--|
| A | 0.90~1.0 | Unweathered, the fracture surface is good and fresh and is contained within fresh bedrock |
| B | 0.90~0.75 | Slightly weathered with good fracture surface, relatively fresh, and the minerals with weak weathering resistance are slightly altered |
| C | 0.75~0.55 | Slightly weathered, the fracture surface is generally smooth and unfilled, and the minerals with weak weathering resistance are partially altered |
| D | 0.55~0.35 | Strongly weathered, poor fracture surface conditions and dense film coverage or angular debris filling on the surface, most minerals with weak weathering resistance are altered |
| E | 0.00~0.35 | Extremely weathered, poor fracture surface conditions with a weak soil film and clay, and most of the minerals with weak weathering resistance are altered |

Table 5 Terms to describe large-scale undulation J_b (Cai et al. 2004)

| Structure type | J_b | Description of volatility (%) |
|----------------|-----------|-------------------------------|
| A | > 3.0 | Interlocking |
| B | 2.5 ~ 3.0 | Stepped |
| C | 2.0 ~ 2.5 | Large undulation |
| D | 1.5 ~ 2.0 | Small to moderate undulation |
| E | < 1.5 | Planar |

μ_{ik} . Referring to previous research results (Li et al. 2013; Zhou et al. 2013; Li et al. 2020a, b), the single-index attribute measurement function of attribute mathematics is shown in Table 8.

Analysis of multi-index comprehensive attribute measurement

The evaluation of the multi-index comprehensive attribute measure is based on the evaluation object with m index values. The multi-index attribute measure analysis can be calculated according to formula (1):

$$\begin{aligned}
 u_{1k} &= \sum_{j=1}^m w_j u_{1jk} \\
 u_{2k} &= \sum_{j=1}^m w_j u_{2jk}
 \end{aligned}
 \tag{1}$$

where u_{1k} is the multi-index attribute of rock mass structure, u_{1jk} is the multi-index attribute of j th rock mass structure, u_{2k} is the multi-index attribute of joint condition, u_{2jk} is the multi-index attribute of j th joint condition, and w is the weight of the j th index.

The judgment matrix is constructed by using the 1 ~ 9 scale method in the analytic hierarchy process (AHP). Through the 9 importance levels and their assignments given by Saaty (1990), the influencing factors in the index system are compared in pairs, and the levels are evaluated according to their importance. Finally, the matrix composed of the comparison results is used as the judgment matrix. The weight vector of the factor is calculated by

the square root method. The evaluation model judgment matrices can be referred to formulas (2) ~ (3):

$$E_1 = \begin{bmatrix} 1 & 3 & 5 \\ \frac{1}{3} & 1 & 3 \\ \frac{1}{5} & \frac{1}{3} & 1 \end{bmatrix}
 \tag{2}$$

$$E_2 = \begin{bmatrix} 1 & \frac{1}{5} & 3 \\ 5 & 1 & 7 \\ \frac{1}{3} & \frac{1}{7} & 1 \end{bmatrix}
 \tag{3}$$

where E_1 is the judgment matrix of rock mass structure, E_2 is the judgment matrix of joint condition.

By finding the eigenvector corresponding to the largest eigenvalue of the judgment matrix, the weights of different index can be obtained. The judgment matrices shown in formulas (2) ~ (3) are used to calculate their eigenvalues and eigenvectors as,

$$\lambda_{\max 1} = 3.0385 \dots \dots \dots B_1 = [0.637, 0.258, 0.105]$$

$$\lambda_{\max 2} = 3.065 \dots \dots \dots B_2 = [0.188, 0.731, 0.081].$$

where $\lambda_{\max 1}$ is largest eigenvalue of the judgment matrix E_1 , B_1 is the weight of the rock mass structure index, $\lambda_{\max 2}$ is largest eigenvalue of the judgment matrix E_2 , B_2 is the weight of the rock mass structure index.

In order to judge whether the weight can be used for multi-index attribute measure analysis or not, the index of consistency ratio (CR) is commonly used in the analytic hierarchy process (AHP) method to test the consistency of the evaluation matrix (Saaty 1990). When $CR < 0.1$, it is generally considered that the degree of the matrix inconsistency is within the allowable range, and the weight can be used for multi-index attribute measure analysis. The CR can be calculated using formula (4):

$$\begin{aligned}
 CR &= \frac{CI}{RI} \\
 CI &= \frac{\lambda_{\max} - n}{n - 1} \\
 CR_1 &= 0.033 < 0.1 \\
 CR_2 &= 0.056 < 0.1
 \end{aligned}
 \tag{4}$$

where CI is the consistency index, RI is the random consistency index, n is the number of non-zero eigenvalues of judgment

Table 6 Terms to describe small-scale undulation J_s (Cai et al. 2004)

| Structure type | J_s | Qualitative index of rock mass characteristics |
|----------------|------------|---|
| A | 3.0 | Very rough, near vertical steps and ridges occur with an interlocking effect on the joint surface |
| B | 2 ~ 3 | Rough, some ridges and steps are evident; asperities are visible; discontinuity surface feels very abrasive (rougher than sandpaper grade 30) |
| C | 1.5 ~ 2 | Slightly rough, asperities on the discontinuity surfaces are distinguishable and can be felt (like sandpaper grade 30-300) |
| D | 0.75 ~ 1.5 | Smooth and polished, surface appears smooth and feels smooth to the touch, visual evidence of polishing exists |
| E | < 0.75 | Slickensided, polished and striated surface that results from sliding along a fault surface or other surface |

Table 7 Indices and criteria for assessment

| Evaluation grade | Structural characteristics of rock mass | | | Feature description of structural plane | | |
|------------------|---|-----------|---------|---|---------|----------|
| | I_1 | I_2 | I_3 | J_1 | J_2 | |
| | RBI | J_L | J_n | AWI | J_B | J_S |
| A | 30~100 | >200 cm | 0.5~1.0 | 0.90~1.0 | >3.0 | >3.0 |
| B | 30~10 | 60~200 cm | 1.0~5.0 | 0.90~0.75 | 2.5~3.0 | 2.0~3.0 |
| C | 10~3 | 20~60 cm | 5.0~10 | 0.75~0.55 | 2.0~2.5 | 1.5~2.0 |
| D | 3~1 | 6~20 cm | 10~15 | 0.55~0.35 | 1.5~2.0 | 0.75~1.5 |
| E | 1~0 | <6 cm | 15~20 | 0.00~0.35 | <1.5 | <0.75 |

matrix, and the value of RI can be taken from Table 9 (Saaty 1990).

The consistency ratios of the rock mass structural characteristics and the structural plane condition evaluation matrix are all calculated to satisfy these two consistency tests.

Analysis of the attribute identification

The purpose of attribute identification is to judge which evaluation level C_k the multiattribute measure of x belongs to. In the attribute comprehensive evaluation, the evaluation set (C_1, C_2, \dots, C_k) is usually an ordered set. For the ordered evaluation set (C_1, C_2, \dots, C_k), determine which evaluation level C_k belongs to x , which can be used as the confidence criterion (Cheng 1997).

Confidence criterion: Suppose (C_1, C_2, \dots, C_k) is an ordered evaluation set of attribute space F , where β is the confidence ranking, and the value range is $0.5 < \beta \leq 1$, usually between 0.6 and 0.7.

When $C_1 > C_2 > \dots > C_k$:

$$k_0 = \min \left\{ k : \sum_{l=1}^k u_{xl} \geq \beta, 1 \leq k \leq K \right\} \quad (5)$$

When $C_1 < C_2 < \dots < C_k$:

$$k_0 = \max \left\{ k : \sum_{l=k}^K u_{xl} \geq \beta, 1 \leq k \leq K \right\} \quad (6)$$

Fortunnel engineering, the worse the quality of the surrounding rock is, the more likely geological disasters will occur. Therefore, the evaluation set (A, B, C, D, E) is an orderly collection, $A < B < C < D < E$. According to the criterion of confidence ranking, $\beta = 0.60$ for calculation in this paper. x is considered to belong to the C_{k_0} level if formula (6) is satisfied.

Identification of GSI attribute interval

According to the above analysis, the attribute interval analysis of the rock mass structure and joint condition can be realized.

Since the attribute space $F = \{A, B, C, D, E\}$ of the rock mass structure and joint conditions correspond to the five rock mass structure intervals and the five joint condition intervals in the GSI value table, the quantitative division of each attribute interval can be realized. As shown in Fig. 2, the method of orthogonal grid lines can be used to realize the comprehensive identification of corresponding GSI attribute intervals.

Attribute quantification model of GSI

The GSI attribute recognition model can determine the GSI value interval. However, the GSI values in the same interval differ by a dozen or more. Thus considering the actual engineering requirements, it is necessary to quantify the GSI values within the same value interval and establish a GSI attribute quantification model.

In the attribute identification model of GSI, according to the concept of confidence criterion in “Analysis of the attribute identification”, when the confidence ranking is greater than 0.6, it is determined that the parameter belongs to the attribute interval. Therefore, for a single interval, the confidence ranking is [0.6, 1]. Therefore, the internal quantification of the same value interval can be realized by linear interpolation with confidence ranking of 0.6 and 1.0 as endpoint values, as shown in Fig. 3. Figure 3 shows that if the confidence ranking is high, the calculated evaluation level of the rock mass is low, and the quality of the rock mass is worse. If the confidence ranking is low, the calculated evaluation level of the rock mass is high, and the quality of the rock mass is better.

In this way, five intervals of rock mass structure characteristics and five intervals of joint conditions intervals can be quantified from the original GSI value table. The attribute quantification model of GSI can be constructed by using orthogonal grid lines. The transformation of GSI values from interval identification to quantitative identification is realized.

Based on the attribute identification model, attribute quantification model and confidence ranking analysis, the multi-index quantification of the geological strength index GSI can be realized through four steps: single-index measurement analysis, multi-index measurement analysis, attribute interval

Table 8 Attribute measurement function of single index (Li et al. 2013; Zhou et al. 2013)

| A | B | C | D | E |
|---|--|--|--|---|
| $u_{111}(t) = \begin{cases} 0 & t < 20 \\ \frac{t-20}{20} & 20 \leq t \leq 40 \\ 1 & t > 40 \end{cases}$ | $u_{112}(t) = \begin{cases} 0 & t < 6.5 \\ \frac{t-6.5}{7} & 6.5 \leq t \leq 13.5 \\ \frac{40-t}{20} & 13.5 < t < 20 \\ 0 & 20 \leq t \leq 40 \end{cases}$ | $u_{113}(t) = \begin{cases} \frac{t-2}{2} & t < 2 \\ 1 & 2 \leq t \leq 4 \\ \frac{13.5-t}{7} & 4 < t < 6.5 \\ 0 & 6.5 \leq t \leq 13.5 \end{cases}$ | $u_{114}(t) = \begin{cases} 0 & t < 0.5 \\ \frac{t-0.5}{1} & 0.5 \leq t \leq 1.5 \\ \frac{4-t}{2} & 1.5 < t < 2 \\ 0 & 2 \leq t \leq 4 \end{cases}$ | $u_{115}(t) = \begin{cases} 1 & t < 0.5 \\ \frac{1.5-t}{0} & 0.5 \leq t \leq 1.5 \\ 0 & t > 1.5 \end{cases}$ |
| $u_{121}(t) = \begin{cases} 0 & t < 1.3 \\ \frac{t-1.3}{1.4} & 1.3 \leq t \leq 2.7 \\ 1 & t > 2.7 \end{cases}$ | $u_{122}(t) = \begin{cases} 0 & t < 0.4 \\ \frac{t-0.4}{0.4} & 0.4 \leq t \leq 0.8 \\ 1 & 0.8 < t < 1.3 \\ \frac{2.7-t}{1.4} & 1.3 \leq t \leq 2.7 \\ 0 & t > 2.7 \end{cases}$ | $u_{123}(t) = \begin{cases} \frac{t-0.13}{0.14} & t < 0.13 \\ 0 & 0.13 \leq t \leq 0.27 \\ 0.27-t & 0.27 < t < 0.4 \\ 0.4 & 0.4 \leq t \leq 0.8 \\ 0 & t > 0.8 \end{cases}$ | $u_{124}(t) = \begin{cases} 0 & t < 0.03 \\ \frac{t-0.03}{0.06} & 0.03 \leq t \leq 0.09 \\ 1 & 0.09 < t < 0.13 \\ \frac{0.27-t}{0.14} & 0.13 \leq t \leq 0.27 \\ 0 & t > 0.27 \end{cases}$ | $u_{125}(t) = \begin{cases} 1 & t < 0.03 \\ \frac{0.09-t}{0} & 0.03 \leq t \leq 0.09 \\ 0 & t > 0.09 \end{cases}$ |
| $u_{131}(t) = \begin{cases} 1 & t < 0.75 \\ \frac{1.25-t}{0.5} & 0.75 \leq t \leq 1.25 \\ 0 & t > 1.25 \end{cases}$ | $u_{132}(t) = \begin{cases} 0 & t < 0.75 \\ \frac{t-0.75}{0.5} & 0.75 \leq t \leq 1.25 \\ 1 & 1.25 < t < 3 \\ \frac{7-t}{4} & 3 \leq t \leq 7 \\ 0 & t > 7 \end{cases}$ | $u_{133}(t) = \begin{cases} \frac{t-3}{4} & t < 3 \\ 1 & 3 \leq t \leq 7 \\ \frac{12.5-t}{5} & 7 < t < 7.5 \\ 0 & 7.5 \leq t \leq 12.5 \end{cases}$ | $u_{134}(t) = \begin{cases} 0 & t < 7.5 \\ \frac{t-7.5}{5} & 7.5 \leq t \leq 12.5 \\ 1 & 12.5 < t < 12.5 \\ \frac{17.5-t}{5} & 12.5 \leq t \leq 17.5 \\ 0 & t > 17.5 \end{cases}$ | $u_{135}(t) = \begin{cases} 0 & t < 12.5 \\ \frac{t-12.5}{5} & 12.5 \leq t \leq 17.5 \\ 1 & t > 17.5 \end{cases}$ |
| $u_{211}(t) = \begin{cases} 0 & t < 0.85 \\ \frac{t-0.85}{0.1} & 0.85 \leq t \leq 0.95 \\ 1 & t > 0.95 \end{cases}$ | $u_{212}(t) = \begin{cases} 0 & t < 0.675 \\ \frac{t-0.675}{0.15} & 0.675 \leq t \leq 0.825 \\ 1 & 0.825 < t < 0.85 \\ \frac{0.95-t}{0.1} & 0.85 \leq t \leq 0.95 \\ 0 & t > 0.95 \end{cases}$ | $u_{213}(t) = \begin{cases} \frac{t-0.45}{0.2} & t < 0.45 \\ 1 & 0.45 \leq t \leq 0.65 \\ \frac{0.825-t}{0.15} & 0.65 < t < 0.675 \\ 0 & 0.675 \leq t \leq 0.825 \\ 0 & t > 0.825 \end{cases}$ | $u_{214}(t) = \begin{cases} 0 & t < 0.25 \\ \frac{t-0.25}{0.2} & 0.25 \leq t \leq 0.45 \\ 1 & 0.45 < t < 0.45 \\ \frac{0.65-t}{0.2} & 0.45 \leq t \leq 0.65 \\ 0 & t > 0.65 \end{cases}$ | $u_{215}(t) = \begin{cases} 1 & t < 0.25 \\ \frac{0.45-t}{0.2} & 0.25 \leq t \leq 0.45 \\ 0 & t > 0.45 \end{cases}$ |
| $u_{221}(t) = \begin{cases} 0 & t < 2.75 \\ \frac{t-2.75}{0.5} & 2.75 \leq t \leq 3.25 \\ 1 & t > 3.25 \end{cases}$ | $u_{222}(t) = \begin{cases} 0 & t < 2.25 \\ \frac{t-2.25}{0.5} & 2.25 \leq t \leq 2.75 \\ 1 & 2.75 < t < 2.75 \\ \frac{3.25-t}{0.5} & 2.75 \leq t \leq 3.25 \\ 0 & t > 3.25 \end{cases}$ | $u_{223}(t) = \begin{cases} \frac{t-1.75}{0.5} & t < 1.75 \\ 1 & 1.75 \leq t \leq 2.25 \\ \frac{2.75-t}{0.5} & 2.25 < t < 2.25 \\ 0 & 2.25 \leq t \leq 2.75 \\ 0 & t > 2.75 \end{cases}$ | $u_{224}(t) = \begin{cases} 0 & t < 1.25 \\ \frac{t-1.25}{0.5} & 1.25 \leq t \leq 1.75 \\ 1 & 1.75 < t < 1.75 \\ \frac{2.25-t}{0.5} & 1.75 \leq t \leq 2.25 \\ 0 & t > 2.25 \end{cases}$ | $u_{225}(t) = \begin{cases} 1 & t < 1.25 \\ \frac{1.75-t}{0.5} & 1.25 \leq t \leq 1.75 \\ 0 & t > 1.75 \end{cases}$ |
| $u_{231}(t) = \begin{cases} 0 & t < 2.5 \\ \frac{t-2.5}{1} & 2.5 \leq t \leq 3.5 \\ 1 & t > 3.5 \end{cases}$ | $u_{232}(t) = \begin{cases} 0 & t < 1.75 \\ \frac{t-1.75}{0.5} & 1.75 \leq t \leq 2.25 \\ 1 & 2.25 < t < 2.5 \\ \frac{3.5-t}{1} & 2.5 \leq t \leq 3.5 \\ 0 & t > 3.5 \end{cases}$ | $u_{233}(t) = \begin{cases} \frac{t-1.25}{0.5} & t < 1.25 \\ 1 & 1.25 \leq t \leq 1.75 \\ \frac{2.25-t}{0.5} & 1.75 < t < 1.75 \\ 0 & 1.75 \leq t \leq 2.25 \\ 0 & t > 2.25 \end{cases}$ | $u_{234}(t) = \begin{cases} 0 & t < 0.375 \\ \frac{t-0.375}{0.75} & 0.375 \leq t \leq 1.125 \\ 1 & 1.125 < t < 1.125 \\ \frac{1.75-t}{0.5} & 1.125 \leq t \leq 1.75 \\ 0 & t > 1.75 \end{cases}$ | $u_{235}(t) = \begin{cases} 1 & t < 0.375 \\ \frac{1.125-t}{0.75} & 0.375 \leq t \leq 1.125 \\ 0 & 1.125 < t < 1.125 \\ 0 & 1.125 \leq t \leq 1.75 \\ 0 & t > 1.75 \end{cases}$ |

Table 9 The value of random consistency index (RI) (Saaty 1990)

| n | 1 | 2 | 3 | 4 | 5 | 6 | 7 | 8 | 9 | 10 | 11 |
|-----|---|---|------|------|------|------|------|------|------|------|------|
| RI | 0 | 0 | 0.58 | 0.90 | 1.12 | 1.24 | 1.32 | 1.41 | 1.45 | 1.49 | 1.51 |

identification, and attribute quantification. Compared with the traditional GSI quantification system, to a certain extent, this new approach overcomes the strong empirical dependence of the GSI, the different quantitative standards, and the variability in the quantitative results. The evaluation index system is more comprehensive, three-dimensional and scientific and can reflect the quality of a rock mass in a wider range. Meanwhile, in terms of obtaining evaluation index parameters, the work of collecting parameters is simplified to a certain extent with this approach, and it has strong applicability. Combined with the characteristics of tunnel construction and considering the tedious work of obtaining indexes, the rock drilling parameters and rock face design parameters in the construction process are selected to simplify the parameter collection work.

Engineering applications

Project profile

The prototype tunnel is an uphill double-track railway tunnel in Dushan Mountain. The area where the tunnel is located is

covered with Quaternary fine breccia soil, crushed stone soil, fragmented stone soil, silty clay, coarse soil, and a debris flow accumulation layer, and the underlying bedrock is Triassic phyllite with sandstone. The surrounding rock of the tunnel is relatively soft, mainly sandstone and phyllite, and locally carbonaceous phyllite. Affected by the regional structure, the rock mass is broken and easy to deform, and joints and fissures have developed. After tunnel excavation, the rock mass is prone to fragmentation, collapse and large deformation.

Engineering geological parameters

According to the requirements of tunnel construction, advanced geophysical prospecting, advance drilling, and tunnel face design are carried out along the entire line of the prototype tunnel.

Based on the design data, the ZDK0+183~ZDK0+263 sections with relatively stable rock structural characteristics are selected for study. According to engineering data, the thickness of the overlying strata is approximately 115 m. At the construction site, two advanced drill holes are arranged at ZDK0+193 and ZDK0+219. The length of each drill hole is 30 m, with

Fig. 2 The attribute identification method of GSI

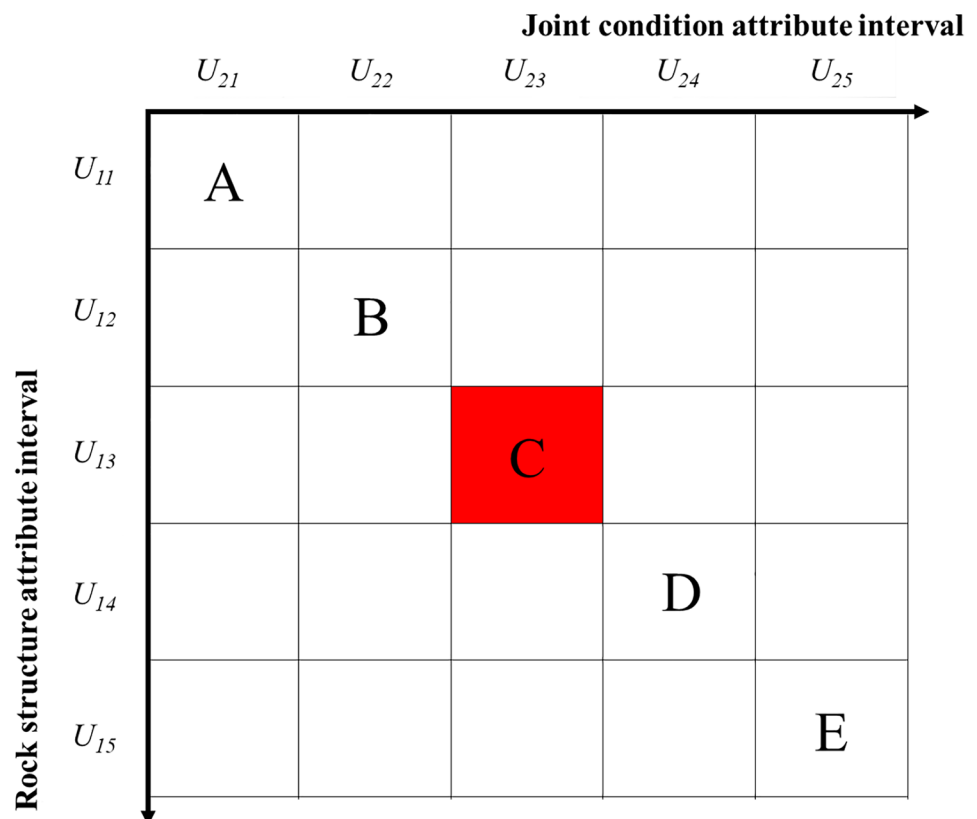
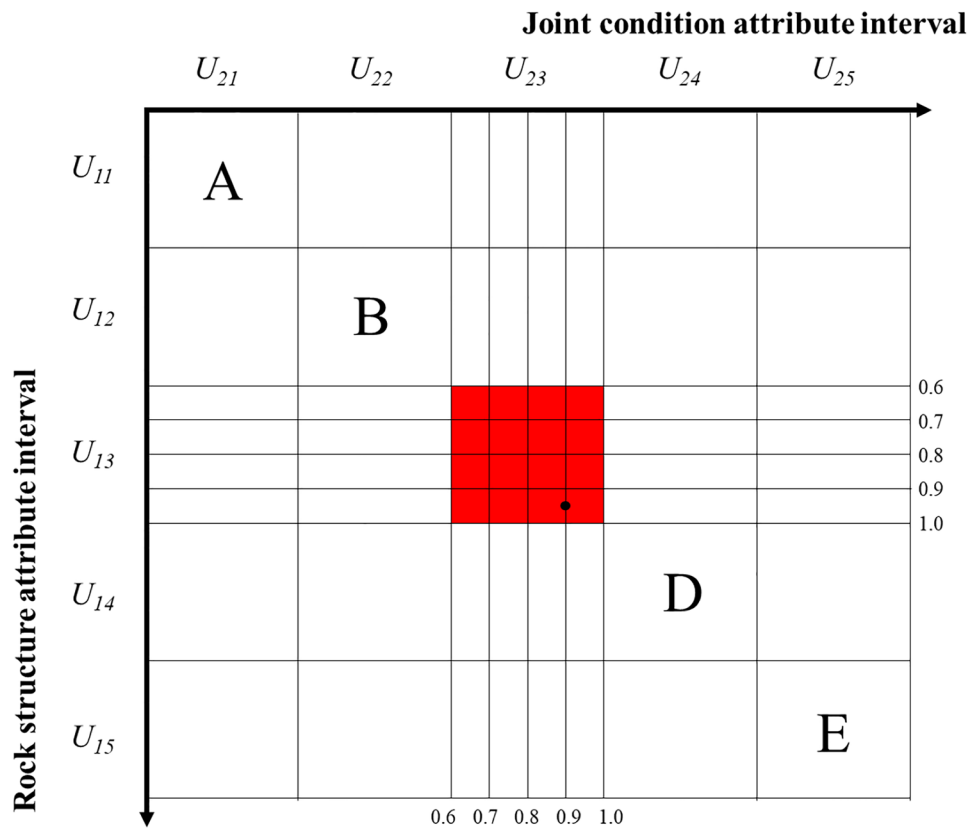


Fig. 3 The attribute quantification method of GSI



an overlapping length of 4 m. Core $RBI_{ZDK0+193}=3.8$ and $RBI_{ZDK0+219}=4.2$ are obtained, and the average value $RBI=4$ is taken. According to the design of the tunnel face, the number of joints is 3. According to Table 2, the score of the joint group is $J_n=5$. According to Table 3, the score of the joint spacing is $J_L=0.37$. According to Table 4, the absolute weathering coefficient is $AWI=0.63$. According to Tables 5 and 6, the large-scale waveform factor is $J_b=2.2$, and the small-scale waveform factor is $J_s=1.8$. Based on geological data, on-site investigations and laboratory tests, the calculation parameters of attribute measures are determined. According to the method presented in this article, the attribute measure is shown in Table 10.

For tunnel engineering, the worse the quality of the surrounding rock is, the more likely geological disasters will

occur. According to the criterion of the confidence ranking, the confidence β for attribute identification is generally between 0.6 and 0.7. In this paper, $\beta=0.60$ is taken for calculation. According to formula (1), the confidence ranking of U_{13} is 0.95, and the confidence ranking of U_{23} is 0.90.

According to the attribute quantification model of the GSI and GSI value table and using the confidence ranking interpolation method, the above calculation results $U_{13}=0.95$ and $U_{23}=0.90$ are used to draw orthogonal lines that intersect at one point, as shown in Fig. 4.

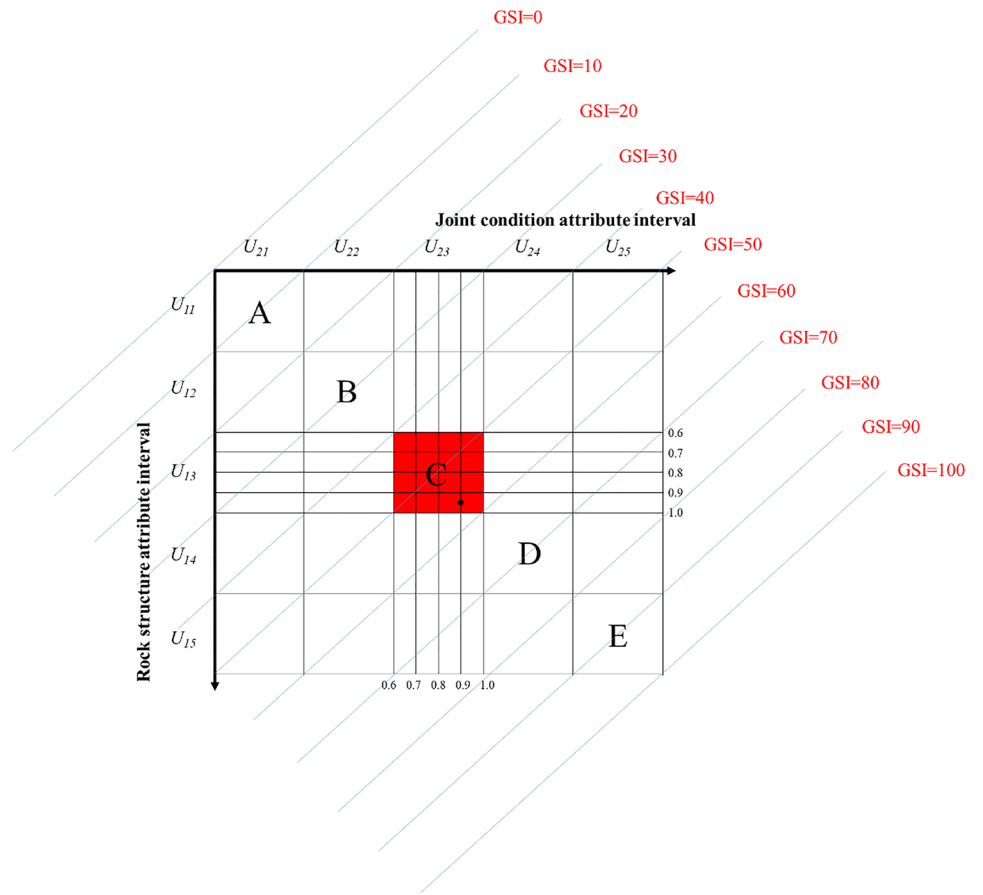
Using the difference in GSI values, the GSI is calculated to be 43 according to formula (7):

$$GSI = 42 + (44 - 42) \times [L_1 / (L_0 + L_1)] = 43 \tag{7}$$

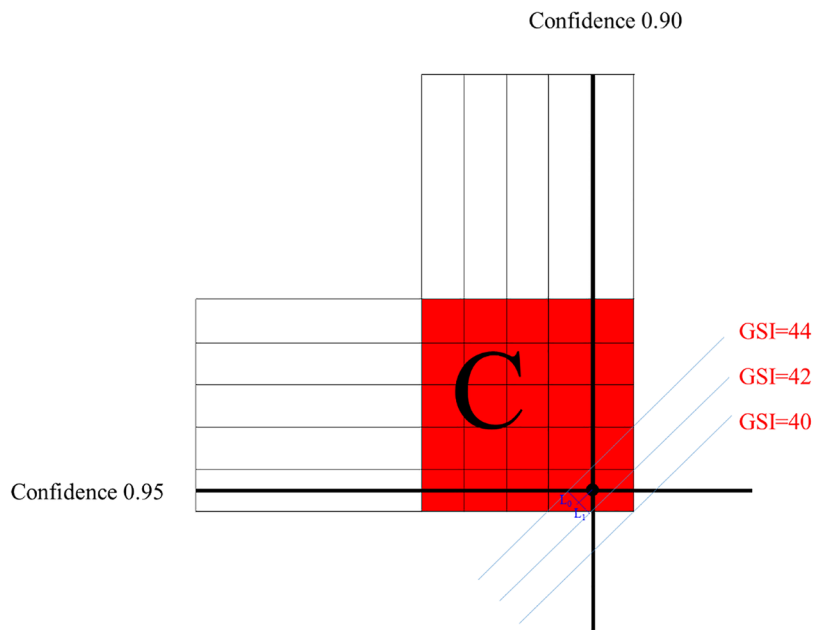
Table 10 Calculation table of attribute measurement

| Evaluation index | Measurements | Attribute measure | | | | |
|------------------|--------------|-------------------|--------------|-------------|--------------|-------------|
| | | A | B | C | D | E |
| I_1 | 4 | 0.00 | 0.00 | 1.00 | 0.00 | 0.00 |
| I_2 | 0.37 | 0.00 | 0.00 | 1.00 | 0.00 | 0.00 |
| I_3 | 5 | 0.00 | 0.50 | 0.50 | 0.00 | 0.00 |
| U_{1k} | | 0.00 | 0.05 | 0.95 | 0.00 | 0.00 |
| J_1 | 0.63 | 0.00 | 0.00 | 0.90 | 0.10 | 0.00 |
| D_1 | 2.20 | 0.00 | 0.00 | 0.90 | 0.10 | 0.00 |
| D_2 | 1.80 | 0.00 | 0.10 | 0.90 | 0.00 | 0.00 |
| U_{2k} | | 0.00 | 0.008 | 0.9 | 0.092 | 0.00 |

Fig. 4 Computing method of GSI



(a) GSI value



(b) Area C GSI value

where L_0 is the distance from this point to the upper value line on GSI, L_l is the distance from this point to the lower value line on GSI.

Numerical analysis model

The steps of establishing a numerical simulation model are as follows:

1. Based on relevant geological data, obtain the values of RBI, J_n , J_L , AWI, J_b , and J_S .
2. Calculate the GSI value based on the above GSI attribute quantification model.
3. According to the equivalent transformation method of the Hoek–Brown strength criterion and Mohr–Coulomb strength criterion, calculate the rock mass parameters.
4. Establish the numerical model based on the obtained rock mass parameters and actual tunnel.

In this numerical analysis model, the Hoek–Brown parameters $m_i \approx 10$, $\sigma_{ucs} = 56.1$ MPa, and $E = 26.2$ GPa were determined by taking the prototype tunnel rock samples and conducting laboratory tests. According to GSI = 43 calculated above and the determination method of the rock mass parameters in the Hoek–Brown criterion, the tensile strength, compressive strength (Hoek et al. 2002), and the Elastic modulus (Hoek et al. 2006) of the rock mass can be calculated using formulas (8)–(13):

$$m_b = m_i \exp\left(\frac{GSI - 100}{28 - 14D}\right) = 1.3059 \tag{8}$$

$$s = \exp\left(\frac{GSI - 100}{9 - 3D}\right) = 0.0017761 \tag{9}$$

$$a = 0.5 + \frac{1}{6} [\exp(-GSI/15) - \exp(-20/3)] = 0.50927 \tag{10}$$

$$\sigma_{cm} = \sigma_{ucs} \frac{[mb + 4s - a(mb - 8s)](mb/4 + s)^{a-1}}{2(1 + a)(2 + a)} = 8.3829 \text{ MPa} \tag{11}$$

$$\sigma_m = \frac{1}{2} \sigma_{ucs} (m_b - \sqrt{m_b^2 + 4s}) = -0.076220 \text{ MPa} \tag{12}$$

$$E_m = E(0.02 + \frac{1 - D/2}{1 + \exp[(60 + 15D - GSI)/11]}) = 5.1285 \text{ GPa} \tag{13}$$

For the tunnel is excellent quality controlled blasting, $D = 0$.

The Hoek–Brown strength criterion is non-linear, so not as easy to use in numerical calculations as linear Mohr–Coulomb parameters. Therefore, the equivalent transformation of the Hoek–Brown strength criterion to Mohr–Coulomb strength parameters has been applied. Hoek et al. (1990, 2002) proposed the calculation method of instantaneous Mohr–Coulomb friction angle φ and cohesion c based on the strength parameter of the Hoek–Brown criterion, as shown in formulas (8)–(9).

$$\sigma_1 = \sigma_3 + \sigma_c \left(\frac{m_b}{\sigma_c} \sigma_3 + s\right)^a \tag{14}$$

$$\alpha = 0.5 \tag{15}$$

$$0 < \sigma_3 < \frac{\sigma_c}{4} \tag{16}$$

$$\sigma_1 = k\sigma_3 + b \tag{17}$$

$$\left. \begin{aligned} k &= \frac{\sum \sigma_1 \sigma_3 - \frac{\sum \sigma_1 \sum \sigma_3}{n}}{\sum \sigma_3^2 - \frac{(\sum \sigma_3)^2}{n}} \\ b &= \frac{\sum \sigma_1 - k \sum \sigma_3}{n} \end{aligned} \right\} \tag{18}$$

According to regression analysis utilizing formulas (8)–(9), the best-fit equivalent Mohr–Coulomb parameters were determined as internal friction angle $\varphi = 22^\circ$ and cohesion $c = 0.18$ MPa. The rock mass mechanical parameters used in the calculation are shown in Table 11.

Using FLAC3D software and relying on the prototype tunnel, the deformation characteristics of ZDK0 + 183 ~ ZDK0 + 263 during construction are simulated and analyzed. The ideal elastoplastic model was used in the calculation, and the yield criterion was the Mohr–Coulomb criterion based on the Hoek–Brown transformation. According to the calculation principle of the underground structure, combined with the actual structural form and geological conditions of the tunnel, the

Table 11 Physical and mechanical parameters

| | Compressive strength (MPa) | Tensile strength (MPa) | Elastic modulus (GPa) | Poisson's ratio | Internal friction angle (°) | Cohesion (MPa) | Unit weight (KN/m ³) |
|----------------------------|----------------------------|------------------------|-----------------------|-----------------|-----------------------------|----------------|----------------------------------|
| Rock masses parameters | 8.4 | 0.08 | 5.1 | 0.32 | 22° | 0.18 | 22.5 |
| Rock parameters | 56.1 | / | 26.2 | 0.32 | 26° | 0.2 | 22.5 |
| Initial support parameters | / | / | 33 | 0.20 | / | / | 23.0 |

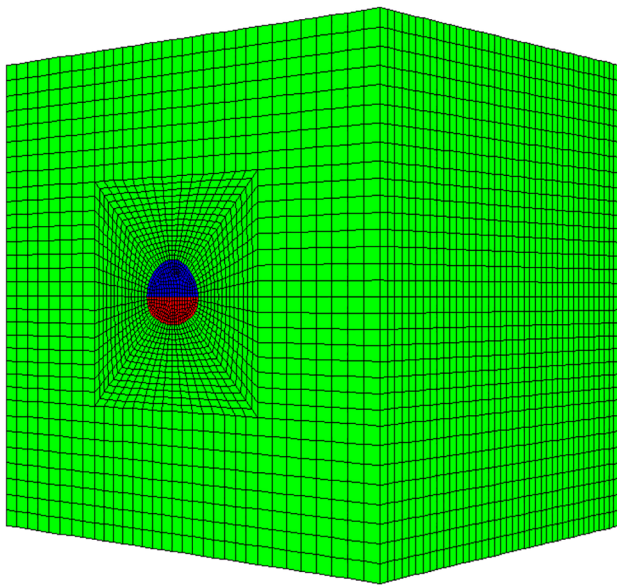


Fig. 5 The calculation model

size of the simulation prototype is as follows: the length in the horizontal direction (x -axis) is 96 m, the length in the vertical direction (y -axis) is 84 m, the cover thickness of the tunnel is 31.88 m, and the length along the tunnel axis direction (z -axis) is 80 m. Under the condition of satisfying the calculation accuracy, the calculation model is established as shown in Fig. 5. The model is divided into 87,658 nodes and 82,920 elements. The grid near the tunnel is relatively dense, and the grid far from the tunnel is relatively sparse, which can better meet the accuracy requirements of the model calculation.

Model boundary conditions and excavation process

According to the design data, the thickness of the overlying strata is 115 m. Based on formula, $\sigma = \lambda h$ the vertical stress is obtained and uniformly applied to the upper surface of the model. The upper surface of the model is set as a free boundary, the normal displacement of the four sides are constrained, and the three-dimensional displacement of the bottom surface is constrained. According to the project construction plan, the tunnel excavation adopts the bench method. The excavation simulation is realized by a null unit. The step length is 8 m, and each excavation footage is 2 m.

In terms of tunnel support, the support timing has a decisive influence on the deformation of the surrounding rock. Judging from the time history of elastic–plastic deformation of the rock surrounding the tunnel, the deformation of the surrounding rock is generally divided into five stages, as shown in Fig. 6. From 0 to t_0 , the surrounding rock is not disturbed by excavation, and the deformation is 0. For $t_0 \sim t_1$,

the surrounding rock is deformed due to the excavation of the adjacent face, and the deformation gradually increases to S_1 . For $t_1 \sim t_2$, when the tunnel face is excavated, the surrounding rock is unloaded and undergoes elastic–plastic deformation, with the deformation reaching S_2 . According to Sun et al. (2011), the duration of this process is approximately 5–20 ms, which can be regarded as instantaneous. For $t_2 \sim t_3$, due to the spatial effect the LDP (longitudinal deformation profile) of the tunnel face excavation, the surrounding rock deformation accumulates and reaches S_3 as the face advances. After t_3 , the surrounding rock deformation is basically stable. Considering the actual situation, the elastic–plastic deformation of the engineering rock mass (the third stage) is completed instantaneously, and the support is difficult to maintain. Therefore, engineering support is mostly applied in the fourth stage. Based on the above analysis, the support simulation adopts a liner unit, which is applied after the rock mass of this cycle is excavated and the calculation is stable. Then, the next cycle excavation is carried out.

Verification of numerical simulation

To compare the difference between the numerical simulation results using rock parameters and rock mass parameters, the numerical simulation results and the on-site monitoring results were compared and analyzed. However, using a single data type (such as vault settlement or headroom convergence) for verification leads to great uncertainty.

It is limiting to use the displacement difference of a single point to measure the rationality of numerical calculation results. The numerical calculation results of rock mass

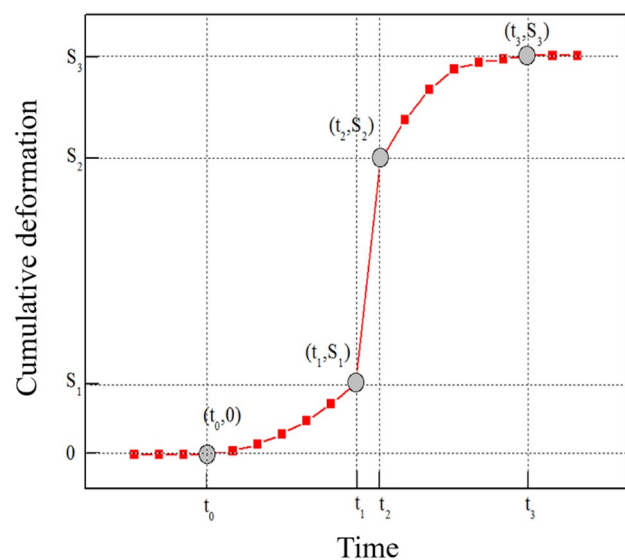
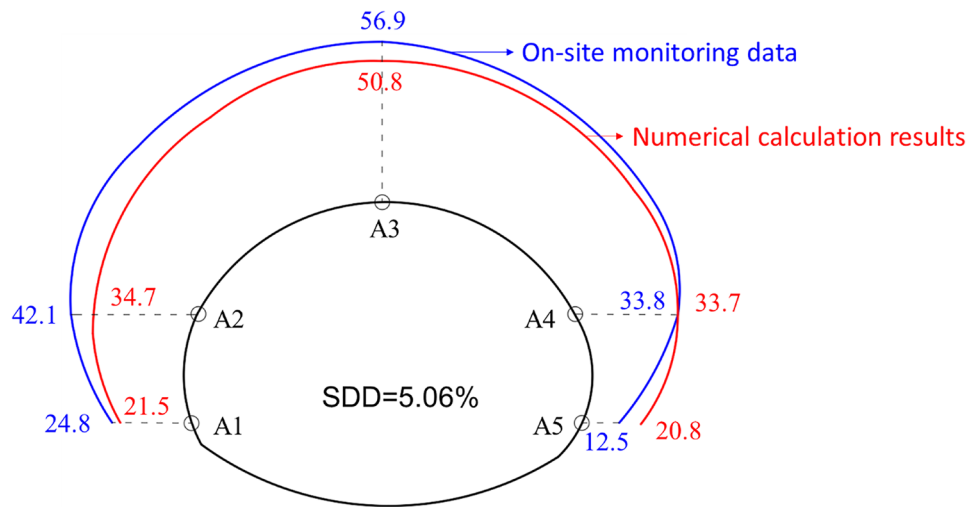


Fig. 6 Three phases of the surrounding rock deformation

Fig. 7 The displacements of section ZDK0+193 using the equivalent rock mass mechanical parameters



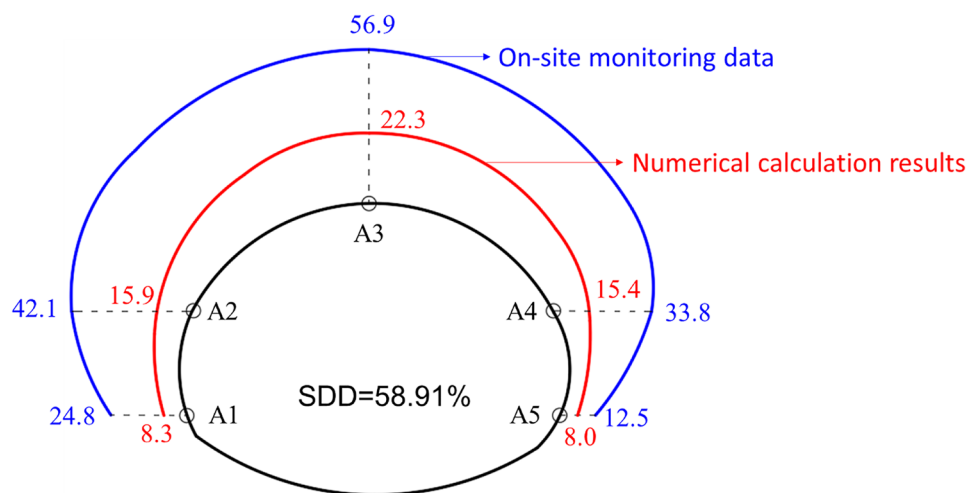
parameters obtained by calculation are compared with the on-site monitoring results, as shown in Fig. 7. The numerical calculation assumes that the parameters of the rock mass are isotropic and that the displacement distribution is symmetric. However, the actual monitoring results show that displacement symmetry does not exist because there are many structural planes or bedding planes in the surrounding rock. To some extent, this leads to some differences between the numerical calculation results and the field monitoring results and some uncertainties. Taking the spandrel as an example, the displacement difference of the left spandrel A2 point is 7.4 mm, while that at the right spandrel A4 point is only 0.1 mm. It is difficult to discuss the asymmetric distribution of displacement caused by rock mass anisotropy, and it is difficult to reflect the overall coincidence degree of equivalent mechanical parameters.

When the displacement difference of a single point is used to measure the rationality of the numerical calculation result, not only is the overall coincidence degree not good,

but an error may even occur. Taking numerical calculation results of rock parameters as an example, the displacement comparison of section ZDK0+193 is shown in Fig. 8. For point A5, the displacement difference of the displacement rock parameters is 4.5 mm, while the calculated deviation of the displacement rock parameters is 8.3 mm. The numerical simulation results of the rock parameters seem to be closer to matching the measured data at point A5. However, comparing Fig. 7 with Fig. 8, the numerical simulation results of the calculated rock mass parameters are obviously more consistent with the actual monitoring data, than when numerical simulation is undertaken solely using the intact rock parameters.

Therefore, to comprehensively measure the rationality of numerical calculation results and reflect the effectiveness of equivalent parameters, this paper proposes a unified treatment method for the displacements of multiple measuring points in a single section. Considering the anisotropy of the rock mass, the cumulative difference between the numerical

Fig. 8 The displacements of section ZDK0+193 using the intact rock mechanical parameters



simulation displacement value and the on-site monitoring displacement value of each measuring point in a single section is divided by the sum of the on-site monitoring displacement values to express the section displacement deviation (SDD).

$$SDD = \frac{\text{sum of difference between the numeral simulation and on-site monitoring displacement}}{\text{sum of the on-site monitoring displacement}} \quad (19)$$

Based on the above principles, the SDD calculated rock mass parameter = 5.06%, while the SDD intact rock parameter = 58.91%. Clearly, the calculated rock mass parameters are closer to the real monitoring values than the intact rock parameters.

From the above results, it can be seen that the GSI quantitative value method based on attribute mathematics and the Hoek–Brown strength criterion can easily and accurately estimate the rock mass mechanical parameters, which has good rationality and applicability in engineering practice.

Conclusion

1. In view of the ambiguity of the GSI index system, considering the structural characteristics of a rock mass and joint conditions, the attribute recognition index system is constructed by introducing the seven indicators of RBI , J_n , J_L , AWI , J_b , and J_s . Applying the multifactor attribute mathematics evaluation theory to GSI system evaluation, a GSI attribute recognition model is constructed to realize GSI attribute interval judgment.
2. Introducing the concept of confidence ranking, using the minimum confidence ranking and the maximum confidence ranking as the endpoint values, the regional quantification of GSI attribute interval is realized by adopting linear interpolation. Furthermore, the attribute quantification model of GSI is constructed, which realizes the transformation from attribute interval acquisition to numerical quantification of the GSI.
3. Aiming at the numerical verification of the GSI attribute quantification model, the inconvenience of numerical simulation based on the Hoek–Brown strength criterion is solved by referring to the equivalent transformation method of the Hoek–Brown strength criterion and Mohr–Coulomb strength criterion. Based on the mechanical analysis of a drilling and blasting tunnel construction process, the problem in the determination of the reinforcement time to support surrounding rock is solved. This approach also solves the ambiguity of matching monitoring data and numerical simulation results in numerical calculations. It can be widely used in engineering applications.

4. In the comparison of on-site monitoring data and numerical simulation results, it is difficult to reflect the overall rationality of the numerical equivalent parameters. Therefore, the concept of SDD is proposed to solve the problem of data mismatch between different monitor-

ing points in the same section due to the discontinuity, heterogeneity and anisotropy of the rock mass. The numerical method verification of the equivalent simulation parameters is realized.

Funding This work was supported by the National Science Fund for Excellent Young Scholars (No. 51722904), National Natural Science Foundation of China (No. 51679131), China Postdoctoral Science Foundation (2019M652383, 2020T130378), and Postdoctoral Innovation Program of Shandong Province (202002008).

References

- Bar N, Barton N (2017) The Q-slope method for rock slope engineering. *Rock Mech Rock Eng* 50:3307–3322
- Barton N (2002) Some new Q-value correlations to assist insite characterisation and tunnel design. *Int J Rock Mech Min Sci* 39:185–216
- Bieniawski ZT (1989) Engineering rock mass classification. New York: Science Press 1989:180–250
- Cai M, Kaiser PK (2006) Visualization of rock mass classification systems. *Geotech Geol Eng* 24:1089–1102
- Cai M, Kaiser PK, Uno H, Tasaka Y, Minami M (2004) Estimation of rock mass deformation modulus and strength of jointed hard rock masses using the GSI system. *Int J Rock Mech Min Sci* 41:3–49
- Cheng Q (1997) Attribute recognition theoretical model with application. *Universitatis Pekinensis, Acta Scientiarum Naturalium* 33(1):12–20 (in Chinese)
- Feng WK, Dong S, Wang Q, Yi XY, Liu ZG, Bai HL (2018) Improving the Hoek–Brown criterion based on the disturbance factor and geological strength index quantification. *Int J Rock Mech Min Sci* 108:96–104
- Hoek E (1990) Estimating Mohr–Coulomb friction and cohesion values from the Hoek–Brown failure criterion. *Int J Rock Mech Min Sci Geomech Abstr* 27(3):227–229
- Hoek E, Carranza-Torres C, Corkum B (2002) Hoek–Brown failure criterion—2002 edition. Hammah R, Bawden W F, Curran J, et al. ed. *Proceedings of the North American Rock Mechanics Society NARMS-TAC 2002*. Toronto: University of Toronto Press, 2002:267–273
- Hoek E, Carter TG, Diederichs MS (2013) Quantification of the geological strength index chart. In: *Proceedings of 47th US Rock Mechanics / Geomechanics Symposium*. San Francisco; 23–26 June
- Hoek E, Brown ET (1997) Practical estimates of rock mass strength. *Int J Rock Mech Min Sci* 34:1165–1186
- Hoek E, Diederichs MS (2006) Empirical estimation of rock mass modulus. *Int J Rock Mech Min Sci* 43:203–215
- Hu XW, Zhong PL, Ren ZG (2002) Rock mass block index and its engineering practice significance. *J Hydraul Eng* 33:80–84 (in Chinese)
- Li LP, Sun SQ, Wang J et al (2020a) Experimental study of the precursor information of the water inrush in shield tunnels due to

- the proximity of a water-filled cave. *Int J Rock Mech Min Sci* 130:104320
- Li LP, Sun SQ, Wang J et al (2020b) Development of compound EPB shield model test system for studying the water inrushes in karst regions. *Tunn. Undergr. Space Technol* 101:103404
- Li SC, Shi SS, Li LP (2013) Attribute identification model and its application of mountain tunnel collapse risk assessment. *J Basic Sci Eng* 21:147–158 (in Chinese)
- Lin DM, Sun Y, Zhang W, Yuan RM, He WT, Wang B, Shang YJ (2014) Modifications to the GSI for granite in drilling. *B Eng Geol Environ* 73:1245–1258
- Marinos P, Hoek E. (2000) GSI: A geologically friendly tool for rock-mass strength estimation. in: *Proceedings GeoEng2000 International Conference on Geotechnical and Geological Engineering*. Melbourne 1422–1446
- Marinos V, Carter TG (2018) Maintaining geological reality in application of GSI for design of engineering structures in Rock. *Eng Geol* 239:282–297
- Russo G (2009) A new rational method for calculating the GSI. *Tunn Undergr Space Technol* 24:103–111
- Saaty TL (1990) How to make a decision: the analytic hierarchy process. *Eur J Oper Res* 48:9–26
- Schlotfeldt P, Carter TG (2018) A new and unified approach to improved scalability and volumetric fracture intensity quantification for GSI and rockmass strength and deformability estimation. *Int J Rock Mech Min Sci* 110:48–67
- Sonmez H, Ulusay R (1999) Modifications to the geological strength index (GSI) and their applicability to stability of slopes. *Int J Rock Mech Min Sci* 36:743–760
- Sonmez H, Ulusay R (2002) A discussion on the Hoek-Brown failure criterion and suggested modifications to the criterion verified by slope stability case studies. *Yerbilim Bull Earth Sci* 26(1):77–99
- Sonmez H, Gokceoglu C, Ulusay R (2004) Indirect determination of the modulus of deformation of rock masses based on the GSI system. *Int J Rock Mech Min Sci* 41:849–857
- Su YH, Feng LZ, Li ZY, Zhao MH (2009) Quantification of elements for geological strength index in Hoek-Brown criterion. *Chin J Rock Mech Eng* 24:103–111 (in Chinese)
- Sun JS, Jin L, Jiang QH, Zhou CB, Lu WB (2011) Study on the loosening mechanism of joint surrounding rock induced by transient stress adjustment during underground blasting excavation. *J Vib Shock* 30:28–34 (in Chinese)
- Winn K, Wong LNY (2019) Quantitative GSI determination of Singapore's sedimentary rock mass by applying four different approaches. *Geotech Geol Eng* 37:2103–2119
- Zhou ZQ, Li SC, Li LP, Shi SS, Song SG, Wang K (2013) Attribute identification model of fatalness assessment of water inrush in karst tunnels and its application. *Rock Soil Mech* 34:818–826 (in Chinese)